ACS central science

Research Article

http://pubs.acs.org/journal/acscii

Fragmentation and Coagulation in Supramolecular (Co)polymerization Kinetics

Albert J. Markvoort,* Huub M. M. ten Eikelder, Peter A. J. Hilbers, and Tom F. A. de Greef*

Computational Biology Group and Institute for Complex Molecular Systems, Eindhoven University of Technology, PO Box 513, 5600 MB Eindhoven, The Netherlands

Supporting Information

ABSTRACT: The self-assembly of molecular building blocks into one-dimensional supramolecular architectures has opened up new frontiers in materials science. Due to the noncovalent interactions between the monomeric units, these architectures are intrinsically dynamic, and understanding their kinetic driving forces is key to rationally programming their morphology and function. To understand the self-assembly dynamics of supramolecular polymerizations (SP), kinetic models based on aggregate growth by sequential monomer association and dissociation have been analyzed. However, fragmentation and coagulation events can also play a role, as evident from studies on peptide self-assembly and the fact that aggregations can be sensitive to mechanical agitations. Here, we analyze how fragmentation and coagulation events influence SP kinetics by theoretical analysis of self-assembling systems of increasing complexity. Our analysis starts with single-component systems in which aggregates are able to grow via an isodesmic or cooperative nucleation−elongation mechanism. Subsequently, equilibration dynamics in cooperative two-component supramolecular copolymerizations are investigated. In the final part, we reveal how aggregate growth in the presence of competing, kinetically controlled pathways is influenced by fragmentation and coagulation reactions and reveal how seed-induced growth can give rise to block copolymers. Our analysis shows how fragmentation and coagulation reactions are able to modulate SP kinetics in ways that are highly system dependent.

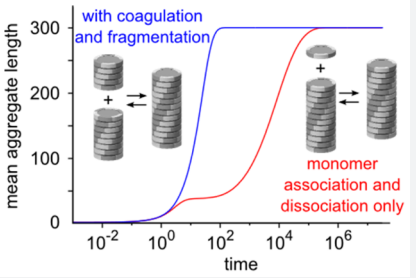

1. INTRODUCTION

One-dimensional self-assembly of molecular components into well-defined supramolecular architectures has opened up new vistas in materials science.[1−7] Currently, applications of these materials are found in the area of biomaterials[8,9] and organic electronics[10−13] while their unique dynamic properties give rise to stimulus responsive materials with self-healing characteristics.[14−16] The rational design of novel materials based on one-dimensional self-assembly requires an exquisite understanding of the molecular mechanisms that govern the formation of these structures. To this end, detailed studies on supramolecular polymerizations under steady-state conditions have revealed how the molecular information encoded in the monomeric units is able to modulate the energetic landscape that controls aggregate growth.[4,17−25] In order to describe changes in the fraction of aggregated material as a function of temperature or concentration, equilibrium models of supramolecular polymerizations typically represent aggregate growth as a sequence of monomer addition steps. Broadly, two limiting mechanims have been described, i.e., an isodesmic mechanism characterized by isoenergetic addition of subsequent monomers to the growing aggregate and a cooperative nucleation−elongation mechanism, where monomer addition to assemblies in the elongation phase is energetically more favorable compared to growth of prenucleus oligomers.[4] These equilibrium models have been expanded to allow (cooperative) coassembly of two components and have subsequently been employed to gain insight into chiral amplification phenomena.[26−30]

Although these detailed studies on supramolecular polymerizations under thermodynamic control have resulted in a better understanding of the molecular features that govern one-dimensional aggregation, recent findings have shown that in many cases kinetically controlled assemblies can be formed.[31−36] These kinetically controlled assemblies often represent different aggregate morphologies, and understanding their equilibration dynamics is key to designing novel materials based on one-dimensional aggregation.[37] In some cases, these kinetically controlled assemblies have been hypothesized to operate via a competitive, parallel operating pathway and equilibrate with thermodynamically stable aggregates via monomer exchange.[33,34,38] In other examples it has been speculated that conversion between different aggregate morphologies occurs via a direct mechanism where one aggregate morphology is slowly transformed into the other.[33,39] Importantly, these additional layers of kinetic control have recently been exploited to engineer supramolecular polymerizations that permit the controlled assembly of multiple components by employing seeded growth of one-dimensional architectures via a true living polymerization mechanism.[40−44] Given the important role of kinetics in one-dimensional self-assembly, a number of recent stud-

Received: January 11, 2016
Published: March 21, 2016

DOI: 10.1021/acscentsci.6b00009
ACS Cent. Sci. 2016, 2, 232−241

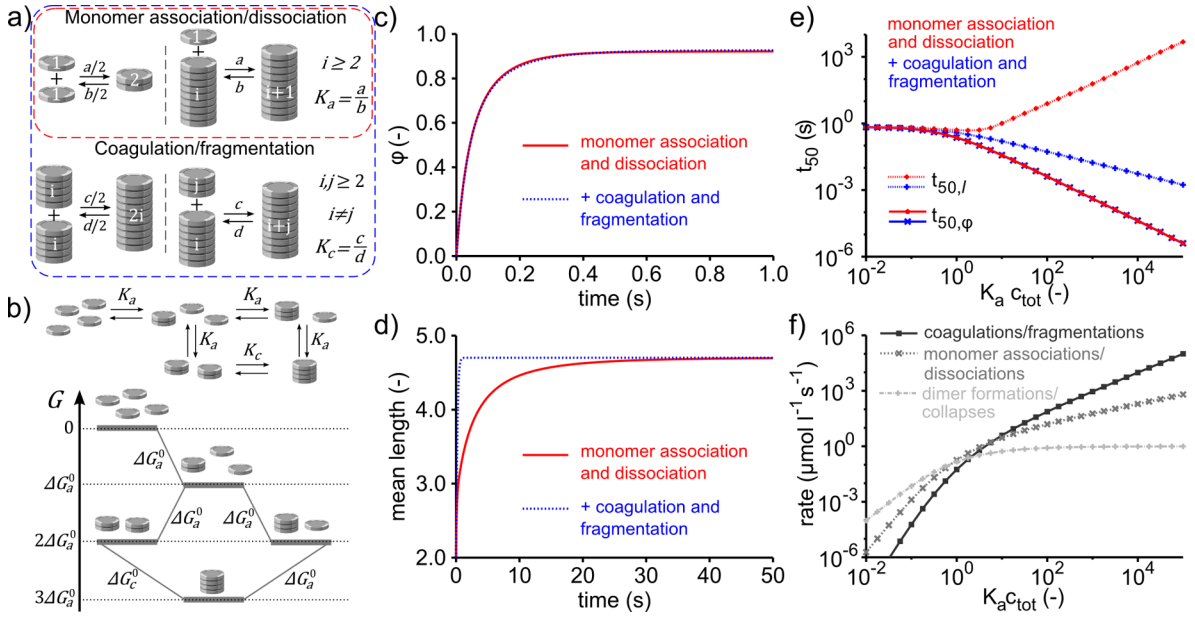

Figure 1. Isodesmic supramolecular polymerization: the role of coagulation and fragmentation on self-assembly kinetics. (a) Coarse-grained reaction diagram of a supramolecular polymerization. One-dimensional aggregation can proceed exclusively via monomer associations and dissociations, or via additional scission and recombination of longer oligomers/polymers (see eqs S4 and S8 in the Supporting Information for a formal description). (b) Reaction and free energy diagram illustrating the formation of a tetramer in the presence of scission and recombination events. For an isodesmic supramolecular polymerization all monomer association equilibrium constants K_a are equal. Wegscheider cyclicity condition states that the rate constants c and d are related via $c/d = a/b$, i.e., $K_c = K_a$. The equivalence of K_c and K_a can also be derived from the energy landscape as the free energy gain upon tetramer formation out of four monomers should be independent of the path followed. (c) Simulated time evolution of the fraction of aggregated material (φ) upon initiation of an isodesmic aggregation from free monomer at a total dimensionless concentration $K_a c_{tot} = 10$. Comparison of $\varphi(t)$ curves shows that addition of coagulation/fragmentation reactions hardly affects the kinetics compared to simulations in which chain growth exclusively occurs by monomer association and dissociation. (d) Time evolution of the mean length of the aggregates using the same parameters as in panel c. The mean polymer length converges much faster to its equilibrium value by the addition of coagulation and fragmentation reactions. (e) The time ($t_{50,\varphi}$) at which 50% of the aggregation process is completed as a function of the concentration does not change by the addition of fragmentation and coagulation reactions. The time ($t_{50,I}$) at which 50% of the mean aggregate length is obtained, however, increases with total concentration when only monomer associations and dissociations occur, whereas it decreases with concentration when scission and recombination of longer oligomers/polymers are also taken into account. (f) Equilibrium rates for different types of reactions as a function of the dimensionless concentration $K_a c_{tot}$. For an isodesmic aggregation mechanism, coagulation and fragmentation reactions are most abundant at $K_a c_{tot} > 1$. All results are obtained from deterministic ODE simulations using $a = c = 10^6$ M^{-1} s^{-1} and $b = d = 1$ s^{-1}.

ies[32−34,39,45−47] have addressed this issue by combining detailed time-dependent spectroscopic studies with increasingly complex kinetic nucleation−elongation models[48−51] that have been developed to describe aberrant protein aggregation. Similar to equilibrium models that describe aggregate distribution in one-dimensional supramolecular polymerizations, the kinetic supramolecular polymerization models employed to date model aggregate growth as a sequence of monomer additions and dissociation events. However, several experimental studies[52,53] have noted that fragmentation of aggregates into two shorter fragments and annealing of small oligomers to larger aggregates can also contribute to overall aggregate growth. Although these fragmentation and coagulation events do not influence the distribution of supramolecular polymers at steady state, they are expected to have a significant influence on aggregation time scales as has been shown by several kinetic studies on for instance amyloid fibrillization[54−58] and wormlike micelle recombination kinetics.[59−63]

Here, we investigate the influence of fragmentation and coagulation events on single and two-component supramolecular polymerizations of increasing mechanistic complexity. We first analyze how these reactions influence the time-dependent self-assembly of single-component systems in which aggregate growth can only follow a single assembly pathway via either an isodesmic or a nucleation−elongation mechanism. Next, we investigate kinetic models of cooperative, two-component systems and reveal how scission and recombination events influence chiral amplification dynamics. Reflecting the increasing importance of kinetically controlled assemblies in one-dimensional supramolecular polymerizations, we next show how fragmentation and coagulation reactions are able to transiently modulate competition between thermodynamically stable aggregates and kinetically controlled species. Finally, the influence of these reactions on seeded supramolecular polymerizations is analyzed and we reveal their effect on the formation of supramolecular diblock copolymers. All models are fully reversible and satisfy the detailed balance condition. Our computational results provide generalizable insights on the role of fragmentation and coagulation reactions in supramolecular polymerizations that can be used to make quantitative predictions of one-dimensional self-assembling systems under different circumstances.

2. RESULTS AND DISCUSSION

2.1. Isodesmic Supramolecular Polymerization. In an isodesmic supramolecular polymerization that exclusively proceeds by monomer association and dissociation events at either end of an aggregate, all monomer association equilibrium constants ($K_a = a/b$) are by definition equal. The kinetics of such a mechanism is described by length independent reaction rate

DOI: 10.1021/acscentsci.6b00009
ACS Cent. Sci. 2016, 2, 232−241

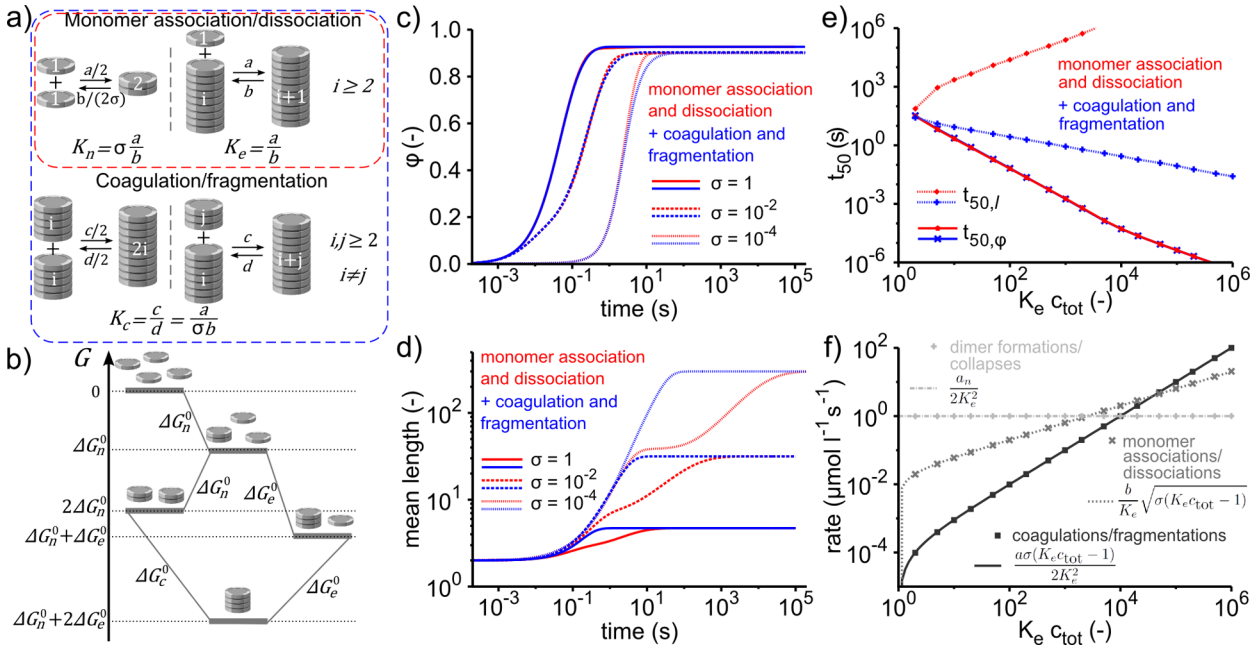

Figure 2. Cooperative supramolecular polymerization: the role of coagulation and fragmentation on self-assembly kinetics. (a) Coarse-grained reaction diagram of a cooperative supramolecular polymerization with a dimeric nucleus size. The equilibrium constant (K_n) of reactions in the nucleation phase are lower compared to the equilibrium constant of reactions in the elongation phase (K_e). The degree of cooperativity is given by the dimensionless cooperativity factor $\sigma = K_n/K_e$. (See eqs S11 and S14 in the Supporting Information for a formal description.) (b) Free energy diagram illustrating the formation of a tetramer in the presence of scission and recombination events. Wegscheider cyclicity condition states that the rate constants c and d are related via $c/d = a/(\sigma b)$. (c) Simulated time evolution of the fraction of aggregated material (φ) upon initiation of a cooperative aggregation from free monomer at a total dimensionless concentration $K_e c_{tot} = 10$ and various values of σ. Comparison of the time traces shows that addition of coagulation/fragmentation reactions has a minor influence on the time evolution. (d) Time evolution of the mean aggregate length for the same values of σ in the absence (red) and presence (blue) of coagulation/fragmentation reactions. In the latter case, this value converges much faster to its equilibrium value and lacks an intermediate plateau for low σ. (e) The time ($t_{50,\varphi}$) at which $\varphi = 0.5$ for a cooperative aggregation mechanism ($\sigma = 10^{-4}$) as a function of $K_e c_{tot}$. This $t_{50,\varphi}$ is insensitive to the addition of scission and recombination events in contrast to the time at which 50% of the mean aggregate length ($t_{50,l}$) is reached which sensitively depends on the presence of coagulation/fragmentation reactions. (f) Rates of the various types of reaction at equilibrium as a function of $K_e c_{tot}$. The results show that for a cooperative mechanism ($\sigma = 10^{-4}$) coagulation/fragmentation reactions are rare and only become abundant at very high $K_e c_{tot}$ (i.e., $>4/\sigma + 1$). Solid lines correspond to analytically derived limit expressions. Results in panels c and d are obtained from deterministic ODE simulations and in panels e and f from stochastic simulations with 10^6 molecules. In all cases $a = c = 10^6$ M^{-1} s^{-1} and $b = 1$ s^{-1}.

constants (red box, Figure 1a; Supporting Information section S1.1 for details). In the second model that we analyze, one-dimensional growth of aggregates may proceed, next to monomer association and dissociation reactions, via additional scission and recombination events (blue box, Figure 1a). In isodesmic supramolecular polymerizations the association equilibrium constants ($K_c = c/d$) describing fragmentation and coagulation reactions are fixed by Wegscheider's cyclicity condition to the monomer association equilibrium constant, i.e., $K_c = K_a$. We illustrate this in Figure 1b for the formation of tetramers employing changes in Gibbs free energies, but the analysis also holds for all other coagulation and fragmentation reactions (see section S1.2 in the Supporting Information). The model is then completely determined by assuming that all noncovalent bonds in the aggregate are equally likely to break, i.e., the fragmentation rate constant d equals the monomer dissociation rate constant b.[64]

The effect of fragmentation and coagulation on isodesmic supramolecular kinetics is investigated by simulating the time evolution of the two models via integration of the corresponding ordinary differential equations (ODEs) using realistic rate constants typical for supramolecular polymerizations (for details see Supporting Information sections S1.1 and S1.3). For an isodesmic aggregation initiated from free monomer at a total dimensionless concentration $K_a c_{tot} = 10$, Figures 1c and 1d show the simulated time evolution of the fraction of aggregated material ($\varphi(t) = \sum_{i=2}^{\infty} i[X_i](t)/c_{tot}$, with $[X_i](t)$ the concentration aggregates of length i at time t) and mean aggregate length ($l(t) = \sum_{i=2}^{\infty} i[X_i](t)/\sum_{i=2}^{\infty} [X_i](t)$), respectively. The analysis shows that, in case aggregate growth only proceeds by monomer association and dissociation, the mean aggregate length equilibrates significantly slower than the fraction of aggregated material. The results further reveal that addition of coagulation and fragmentation reactions hardly affects the equilibration time of $\varphi(t)$ compared to the situation in which aggregate growth exclusively occurs by monomer association and dissociation. Strikingly, when we compare the time evolution of the mean aggregate length ($l(t)$), addition of coagulation and fragmentation reactions appears to dramatically accelerate the convergence of $l(t)$ toward its equilibrium value.

In order to understand the concentration-dependent kinetics of isodesmic supramolecular polymerizations, we calculated the time at which the degree of polymerization ($t_{50,\varphi}$) and the mean aggregate length ($t_{50,l}$) reach 50% of their equilibrium values for several values of the dimensionless concentration. As depicted in Figure 1e, the presence of fragmentation and coagulation hardly affects the concentration dependence of $t_{50,\varphi}$. In contrast, the dependence of $t_{50,l}$ on concentration changes significantly upon addition of coagulation and fragmentation reactions. When aggregate growth occurs by monomer association and

DOI: 10.1021/acscentsci.6b00009
ACS Cent. Sci. 2016, 2, 232−241

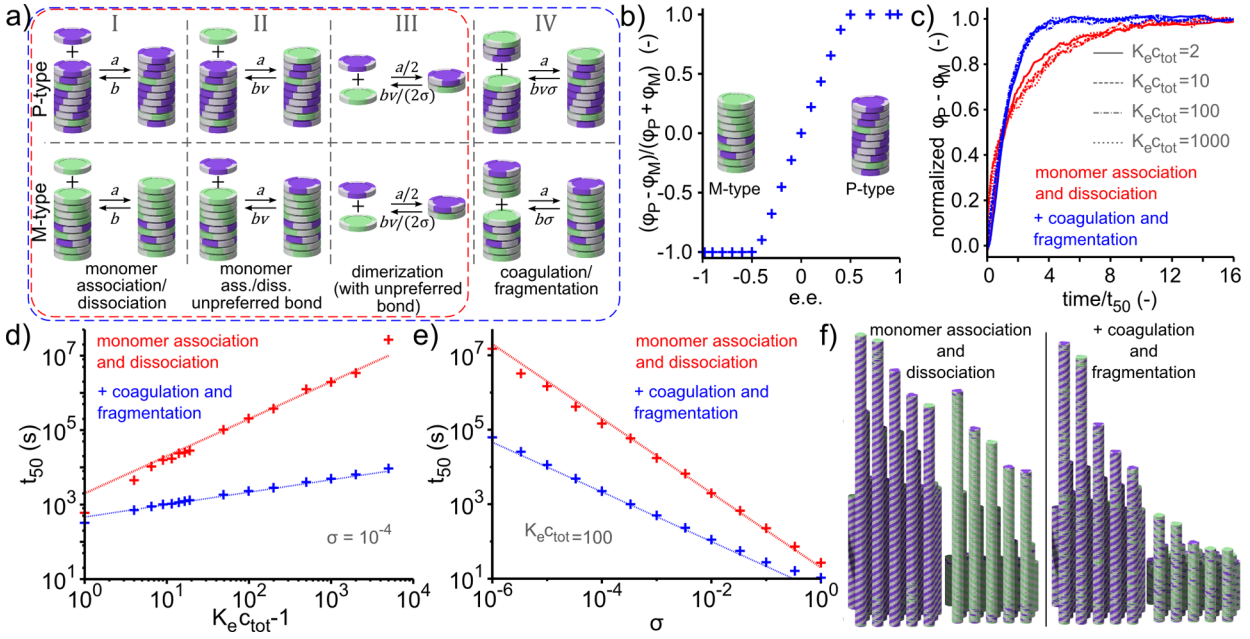

Figure 3. The influence of fragmentation and coagulation on cooperative supramolecular copolymerizations kinetics: majority rules. (a) Coarse-grained reaction diagram of a cooperative supramolecular copolymerization where two enantiomers can self-assemble into aggregates of two opposite helicities. One enantiomer (purple) prefers right-handed helical aggregates (P) while the other (green) prefers the opposite helicity (M). The cooperativity is described by σ, and we assume a dimeric nucleus size. Rate constant for dissociation of a monomer present in an aggregate corresponding to its unpreferred helicity is increased by a factor ν. (See eqs S27−S29 in the Supporting Information for a formal description.) (b) Illustration of the majority rules principle: the curve showing the net helicity, i.e., fraction of molecules in P-type helical aggregates (φ_P) minus the fraction in M-type helical assemblies (φ_M), as a function of the enantiomeric excess (ee) under steady-state conditions, is nonlinear. (c) Simulated time evolution of the net helicity at ee = 0.2 and $\sigma = 10^{-4}$ for four values of the dimensionless concentration $K_e c_{tot}$. Supramolecular copolymerization is initiated by mixing the two enantiomerically related monomers at time $t = 0$. The net helicity is scaled by its initial and final values while time is scaled by t_{50}, i.e., the time at which the scaled net helicity equals 0.5. Concentration-dependent curves corresponding to the same growth mechanisms collapse on a single master curve. Corresponding unscaled curves are shown in Figure S13. (d) t_{50} as a function of the reduced dimensionless concentration $K_e c_{tot} - 1$. The two lines show the analytical fits, i.e., $t_{50} = (K_e c_{tot} - 1)/(5b\sigma)$ for monomer association and dissociation and $t_{50} = (K_e c_{tot} - 1)^{1/3}/(b\sigma^{2/3})$ with addition of coagulation/fragmentation reactions. (e) t_{50} as a function of the cooperativity factor σ for a dimensionless concentration $K_e c_{tot} = 100$ and ee = 0.2. Lines correspond to the same formulas as in part d. Underlying kinetic curves are shown in Figure S14. (f) Snapshots of simulations with 10^4 molecules (see Movie 4) at t = 200 s show that the presence of coagulation and fragmentation highly accelerates majority rules kinetics because the mixing of enantiomers inside aggregates no longer exclusively proceeds from the ends. Results are obtained with stochastic simulations of, unless stated otherwise, 10^6 molecules, $a = 10^6$ M^{-1} s^{-1}, $b = 1$ s^{-1}, $c_{tot} = 100$ μM, and $\nu = 2$.

dissociation reactions only, $t_{50,l}$ increases for higher values of $K_a c_{tot}$. However, addition of coagulation and fragmentation events results in a decrease in $t_{50,l}$ as a function of the dimensionless concentration, indicating that equilibration of the mean aggregate length is actually faster at higher total concentrations or larger values of K_a. Figure 1f depicts the rates of the different reaction types—monomer associations and dissociations, dimer formations and collapses, and coagulation and fragmentation events—at steady state as a function of the reduced concentration. In the region of spontaneous growth, i.e., $K_a c_{tot} > 1$, coagulation and fragmentation events are most abundant.

Apart from integration of the ODEs, the aggregation kinetics of isodesmic supramolecular polymerizations can also be analyzed using kinetic Monte Carlo simulations (Supporting Information sections S1.1 and S1.3). These stochastic simulations corroborate the main findings of the ODE analysis and provide an excellent visualization tool to capture the mechanism dependent kinetics of isodesmic supramolecular polymerizations (Movies 1 and 2).

2.2. Cooperative Supramolecular Polymerization. Next, we investigated the effect of fragmentation and coagulation events in self-assembling systems where one-dimensional aggregate growth occurs via a cooperative nucleation−elongation mechanism.[49] In a cooperative nucleation−elongation mechanism with a dimeric nucleus, the association equilibrium constants of subsequent monomer associations and dissociations are related by $K_n = K_1 < K_2 = K_3 = ... = K_e$ with the cooperativity factor σ defined as K_n/K_e. First we analyze a kinetic nucleation−elongation model in which aggregate growth exclusively occurs by monomer association and dissociation. The corresponding rate equations are identical to the isodesmic case with the exception that the rate constant for dimer dissociation is multiplied by σ^{-1} (Figure 2a). We compare this model to a second model in which chain growth may proceed additionally via scission and recombination events. For this cooperative nucleation−elongation mechanism the reaction cycles in the presence of fragmentation and coagulation events imply that the association equilibrium constants K_c describing fragmentation and coagulation reactions are related to K_e via $K_c = K_e^2/K_n = K_e/\sigma$. In terms of changes in Gibbs free energies this relation may be interpreted (Figure 2b) as a free energy gain ΔG_e upon formation of a new noncovalent bond and a free energy penalty $-RT \ln(\sigma)$ upon production of a new aggregate, independent whether the new aggregate originates from dimerization of two monomers or from scission of an existing assembly. The kinetic model is then fully determined by fixing the backward rate constants, i.e., $c = a$ and $d = b\sigma$.

DOI: 10.1021/acscentsci.6b00009
ACS Cent. Sci. 2016, 2, 232−241

Time traces of the degree of polymerization ($\varphi(t)$) and the mean aggregate length ($l(t)$) upon initiation from free monomer at $K_e c_{tot} = 10$ are shown in Figures 2c and 2d, respectively. Curves are provided for three values of the cooperativity factor σ both for the case in which aggregate growth exclusively occurs by monomer associations and dissociations and for the case when coagulation and fragmentation events are also taken into account. The rate at which $\varphi(t)$ equilibrates decreases with increasing cooperativity (smaller σ) and reduces slightly further by addition of coagulation and fragmentation events. Moreover, the recombination events dramatically accelerate the convergence of the mean aggregate length to its equilibrium value, as after depletion of the initial monomer pool in the absence of these coagulation events the initially formed oligomers (Figure S17) can only grow after monomer dissociation from other oligomers. And this speedup due to recombination events is more significant for smaller values of σ, i.e., when aggregate growth is more cooperative.

Analysis of $t_{50,\varphi}$ and $t_{50,l}$ as a function of the total dimensionless concentration (Figure 2e) shows that, analogous to the isodesmic case, the presence of fragmentation and coagulation reactions in a nucleation−elongation mechanism hardly affects $t_{50,\varphi}$ while it inverts the concentration dependence of $t_{50,l}$. For an aggregation proceeding exclusively via monomer associations and dissociations $t_{50,l}$ increases linearly with both the reduced concentration and the inverse of the cooperativity factor ($1/\sigma$) (Figure S9). In contrast, in the presence of coagulation and fragmentation reactions $t_{50,l}$ scales with the square root of both the reduced concentration and the cooperativity.

Similar to the isodesmic mechanism, we analyzed the steady-state rates of the different reaction types as a function of the total concentration for a moderately cooperative system ($\sigma = 10^{-4}$, Figure 2f). Compared to an isodesmic mechanism, coagulation and fragmentation events at steady state occur orders of magnitude less frequently. Moreover, at low and intermediate dimensionless concentrations ($1 < K_e c_{tot} < 1/\sigma$) the order of the steady-state rates for the different reaction types is inverted in comparison to an isodesmic aggregation mechanism at the same concentration. In this concentration regime, formation and dissociation of dimeric nuclei are the most frequently occurring reactions while fragmentation and coagulation reactions are least frequent. Analytical expressions for the equilibrium rates of the different reaction types (derived in Supporting Information section S2 based on the assumption that in equilibrium the monomer concentration is approximately $1/K_e$) closely match the rates obtained from stochastic simulations (Figure 2f) as well as the rates obtained by solving the deterministic rate equations truncated at sufficiently high polymer length (Figure S8). According to the analytical expressions, the steady-state rate of fragmentation and coagulation reactions scales linearly with the cooperativity factor σ while the steady-state rate of monomer associations and dissociations scales with the square root of σ. Consequently, aggregations characterized by a higher cooperativity (smaller σ) display significantly fewer fragmentation and coagulation events, however, the presence of these reactions significantly accelerates the equilibration of the mean aggregate length (Movie 3).

2.3. Supramolecular Copolymerization. Next, we extended our analysis to understand the effect of fragmentation and coagulation events on the coassembly kinetics of two components that can assemble into two different aggregate types. When the two components are enantiomerically related and their corresponding aggregates differ in helicity, a slight excess of one enantiomer can lead to a strong bias toward coassemblies with the helicity corresponding to the major enantiomer, a phenomenon known as the majority rules principle.[65] We have previously modeled[29,30] this chiral amplification phenomenon by considering the supramolecular copolymerization of two enantiomers *R* and *S*, where the *R* enantiomer prefers right-handed helical aggregates P while the *S* enantiomer prefers assemblies with the opposite handedness M (Figure 3a). This analysis revealed that the helical bias as a function of the enantiomeric excess (ee) at equilibrium (Figure 3b) is fully described by the cooperativity factor σ and an additional mismatch free energy (MMP) which penalizes addition of a monomer to aggregates of its unpreferred helicity. Here we use stochastic simulations extended with coagulation and fragmentation events (Supporting Information sections S1.4 and S1.5) to investigate the effect of these reactions on majority rules kinetics. In terms of rate constants the helical preference is achieved by multiplying the backward rate constants with a factor $\nu = \exp(-\mathrm{MMP}/RT)$ when monomers and oligomers dissociate from their nonpreferred aggregate type (Figure 3a).

To simulate the kinetics of a majority rules experiment initiated by mixing of pre-equilibrated homochiral aggregates, we first simulate the cooperative assembly of the *R* and *S* enantiomers in isolation until steady state is reached. Next, the two systems of equilibrated homochiral aggregates are combined at $t = 0$ and the supramolecular copolymerization is followed in time. Both for the case in which coassembly exclusively occurs by monomer association and dissociation and the case where additionally coagulation and fragmentation events occur, the time evolution of the net helicity upon mixing at a 3:2 ratio is followed for four different concentrations (Figure S13). Figure 3c displays the scaled net helicity as a function of the t/t_{50} with t_{50} the time at which the net helicity reaches a value of 0.5. Interestingly, the shapes of the scaled curves appear independent of the total concentrations, but distinctive on the presence or absence of coagulation and fragmentation reactions.

In order to gain more insight into the kinetics of the majority rules effect, we investigate the dependence of t_{50} on the total concentration, cooperativity, and enantiomeric excess. Independent of the contribution of fragmentation and coagulation reactions, t_{50} increases with the reduced concentration (Figure 3d, ee = 0.2 and $\sigma = 10^{-4}$). However, the dependence on the concentration is linear when aggregate extension occurs exclusively by monomer associations and dissociations, while t_{50} only increases with the cube root of the concentration when growth can additionally occur by coagulation and fragmentation events. A clear relationship is also observed between t_{50} and the cooperativity factor σ, where the exact relationship again depends on the presence of scission and recombination events (Figure 3e). In contrast, the ee hardly affects t_{50} as long as the ee remains below a critical value, corresponding to a situation where aggregates of both helicities can persist (Figure S15). Together these observed dependencies result in the formulas depicted in Figures 3d and 3e along with the data, i.e., $t_{50} = (K_e c_{tot} - 1)/(5b\sigma)$ for the case when aggregate growth occurs exclusively by monomer association and dissociation and $t_{50} = (K_e c_{tot} - 1)^{1/3}/(b\sigma^{2/3})$ for the case when additionally coagulations and fragmentations are also present. Importantly, our analysis thus shows that the concentration dependence of t_{50} in a majority rules experiment is a reliable indicator of the presence of fragmentation and coagulation reactions.

Comparison of the t_{50} dependencies on concentration and cooperativity (Figures 3d and 3e) further reveals that the

DOI: 10.1021/acscentsci.6b00009
ACS Cent. Sci. 2016, 2, 232−241

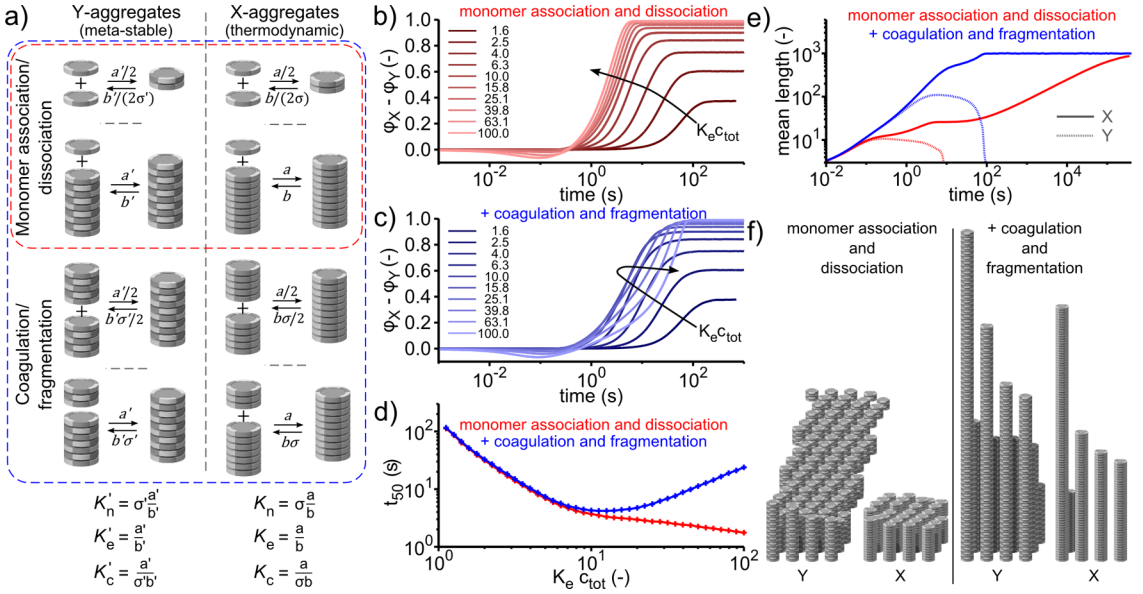

Figure 4. The influence of fragmentation and coagulation on self-assembly kinetics in the presence of a competing pathway. (a) Coarse-grained reaction diagram of a cooperative supramolecular polymerization of a single monomer type into thermodynamically favored X-type aggregates in the presence of a kinetically controlled, parallel operating pathway producing Y-type aggregates. In both pathways cooperative aggregation occurs via a nucleation−elongation mechanism with a dimeric nucleus size. Rate constants a and b and cooperativity factor σ correspond to the formation of stable on-pathway aggregates while the formation of off-pathway aggregates is controlled by a', b', and σ'. (See eq S23 in the Supporting Information for a formal description.) (b) Simulated time evolution of the fraction of polymerized material in X-type aggregates (φ_X) minus the fraction of polymerized material in Y-type assemblies (φ_Y) when a cooperative supramolecular polymerization only proceeds via monomer associations and dissociations and is initiated from free monomer. Curves represent different total concentrations. (c) Idem for the case where aggregation can proceed additionally via recombination and scission events. (d) The time (t_{50}) at which $\varphi_X - \varphi_Y$ reaches 50% of its equilibrium value as a function of the dimensionless concentration. Whereas for MR the kinetics at higher concentrations was increased by orders of magnitude due to the presence of fragmentation and coagulation reactions, here these reactions slow down the formation of thermodynamically stable aggregates. (e) Simulated time evolution of the mean lengths of on- and off-pathway aggregates at $K_e c_{tot} = 100$. Addition of fragmentation and coagulation reactions results in the formation of longer aggregates of the metastable product. (f) Snapshots of simulations with 2000 molecules (see Movie 5), $K_e c_{tot} = 50$, $\sigma = 10^{-2}$, and $\sigma' = 2.5 \times 10^{-3}$ at $t = 5$ s show that the rapid formation of longer metastable aggregates in the presence of coagulation and fragmentation reactions hinders the formation of thermodynamically stable assemblies. Results are obtained with stochastic simulations of, unless stated otherwise, 10^6 molecules, $a = 10^6$ M^{-1} s^{-1}, $b = 1$ s^{-1}, $\sigma = 10^{-4}$, $a' = 10^6$ M^{-1} s^{-1}, $b' = 5$ s^{-1}, and $\sigma' = 6.67 \times 10^{-4}$.

addition of fragmentation and coagulation significantly increases the equilibration kinetics in majority rules experiments. This is corroborated by Movie 4 (with snapshots in Figure 3f), which compares two kinetic simulations of majority rules experiments: one in the absence and one in the presence of fragmentation and coagulation. In the absence of concentration dependent data, the formulas for t_{50} still allow for comparison to the experimental observation that mixing two 20 μM solutions of enantiomerically related benzene-1,3,5-tricarboxamide (BTA) in methylcyclohexane leads to the setting of a new equilibrium within 1 min at room temperature.[28] With previously determined thermodynamic parameters for this system ($K_e = 1.4 \times 10^6$ M^{-1} and $\sigma = 4.5 \times 10^{-6}$ at 293 K)[29] and diffusion controlled association forward rate constants a of 10^9 M^{-1} s^{-1}, the formulas predict a t_{50} of 20 min (corresponding to a 90% completion time of roughly 2 h) for a coassembly that exclusively occurs by monomer associations and dissociations versus a t_{50} of 11 s for a polymerization including fragmentation and coagulation. Of the two models only the kinetic model that incorporates fragmentation and coagulation events can thus explain the observed experimental time scales.

2.4. Pathway Complexity. A key factor in supramolecular polymerization kinetics is the possible presence of competing aggregation pathways. We have previously shown that when monomers can assemble into thermodynamically stable aggregates as well as into metastable aggregates via a kinetically controlled, parallel operating pathway, key signatures of the supramolecular polymerization kinetics are an initial excess of metastable product and an inverted dependence of t_{50} at high monomer concentrations caused by transient buffering of monomers in metastable aggregates.[32] Although both of these features could be explained by a kinetic model based on successive monomer associations and dissociations, here we investigate the effect of additional coagulation and fragmentation events on a supramolecular polymerization featuring this pathway complexity. The reaction scheme examined (Figure 4a) assumes two parallel pathways in which cooperative aggregation may occur via a nucleation−elongation mechanism with a dimeric nucleus size and no direct interconversion beween the two types of aggregates. In particular, we consider X-type aggregates identical to those of the single pathway cooperative supramolecular polymerization above ($\sigma = 10^{-4}$) and Y-type aggregates that are slightly less cooperative ($\sigma' = 6.67 \times 10^{-4}$) and metastable due to an elongation equilibrium constant for monomer association (K_e') that is one-fifth of the elongation equilibrium constant for the X-type aggregates (K_e).

The time evolution of the fraction of polymerized material in stable X-type aggregates (φ_X) minus the fraction of polymerized material in metastable Y-type assemblies (φ_Y) as obtained from stochastic simulations is illustrated in Figure 4b for the case when aggregate growth only proceeds via monomer associations and dissociations and is initiated from the free monomer. The simulations reveal that the time needed for $\varphi_X - \varphi_Y$ to equilibrate

DOI: 10.1021/acscentsci.6b00009
ACS Cent. Sci. 2016, 2, 232−241

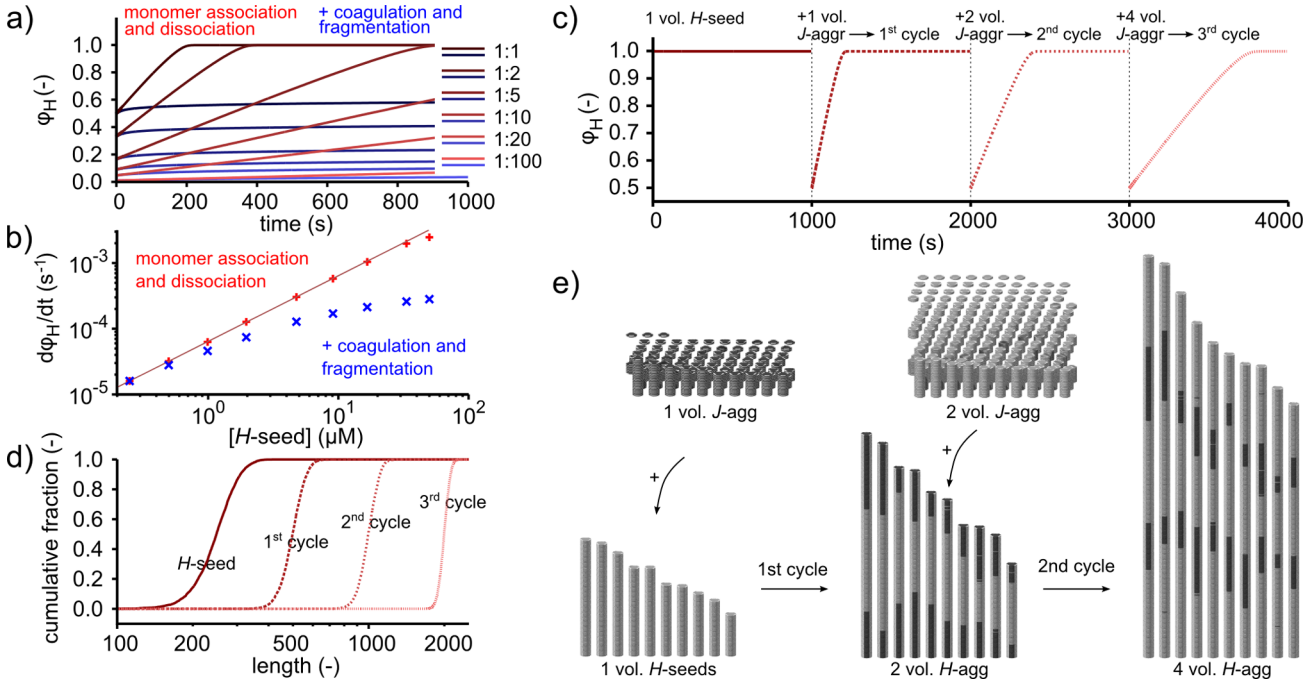

Figure 5. Self-assembly kinetics of seeded supramolecular polymerizations in the presence of competing pathways. (a) Simulated time evolution of the fraction of molecules in cooperative H-aggregates (φ_H) upon addition of H-aggregate seeds of length 250 to a system of kinetically trapped isodesmic J-aggregates consisting of 10^6 monomers. The legend indicates the ratio between the numbers of monomers in the seeds and in the metastable isodesmic system, while line color indicates the growth mechanism. (b) Log–log plot of the rate of increase in φ_H during the initial 200 s as a function of seed concentration after mixing. The linear relationship (slope 1.00) in case aggregation proceeds exclusively via monomer associations and dissociations indicates that the supramolecular polymerization is first order with respect to the seed concentration. In case also fragmentation and coagulation events are enabled, the H-aggregate growth rate is much lower due to rapid reduction in number of seeds resulting from their recombination, especially for higher seed concentrations. (c) Simulated time evolution of φ_H when polymerization proceeding exclusively via monomer associations and dissociations is initiated from 4000 H-seeds of length 250 and every 1000 s one equivalent of equilibrated J-aggregates is added. The rate of supramolecular polymerization decays exponentially with base 0.5 as no new H-aggregates are nucleated in the time scale of the experiments and mixing halves the concentration of existing H-aggregates each cycle. (d) Cumulative histograms of length distributions of H-aggregates at the end of each cycle. Each cycle the mean length of the aggregates roughly doubles, which can be associated with a blockwise growth of the aggregates. (e) Snapshots of stochastic simulations (see Movie 6) with 10^3 molecules per 1 vol showing two cycles of J-aggregate addition to H-seeds, with initial length 100, corroborate the blockwise growth. Molecules added in different cycles are identical though colored distinctly for visualization purposes. All results are obtained from stochastic simulations with $a = 10^6$ M^{-1} s^{-1}, $b = 0.1$ s^{-1}, $\sigma = 10^{-9}$, $a' = 10^6$ M^{-1} s^{-1}, $b' = 1$ s^{-1}, $\sigma' = 1$, and $c_{tot} = 100$ μM.

decreases monotonically with the total concentration for this choice of parameters while the (relative) amount of metastable assemblies increases with the concentration. For the highest concentrations considered, excessive formation of metastable assemblies is evidenced from the negative values of $\varphi_X - \varphi_Y$ in the initial part of the simulations. The analogous time evolutions for the case where aggregation may proceed additionally via recombination and scission events (Figure 4c) show the same excessive formation of metastable product for the higher concentrations. However, instead of monotonically decreasing with the concentration, the time needed for $\varphi_X - \varphi_Y$ to equilibrate now reaches a minimum at an intermediate concentration while for higher concentrations the equilibration kinetics slows down due to buffering of the monomer pool by metastable assemblies (vide infra). The concentration-dependent delay in formation of thermodynamically stable assemblies is outlined in Figure 4d, where both for the case with and for the case without fragmentation and coagulation, the time (t_{50}) at which $\varphi_X - \varphi_Y$ reaches 50% of its equilibrium value is depicted as a function of the total monomer concentration. The inversion in the concentration dependence of t_{50} that we earlier already attributed to the existence of a kinetically controlled competing pathway is thus obtained for a wider parameter regime in the presence of fragmentation and coagulation events. Moreover, in the presence of fragmentation and coagulation events the inversion in the concentration dependence of t_{50} can coincide with a slight excess of metastable product formation, in correspondence with the experimental observation.[32]

In contrast to the (orders of magnitude) increase in majority rules kinetics due to fragmentation and coagulation reactions (vide supra), here these reactions dramatically delay the formation of thermodynamically stable aggregates. To understand this effect in detail, we plotted the simulated time evolution of the mean lengths of on- and off-pathway aggregates at $K_e c_{tot} = 100$ (Figure 4e), i.e., at the concentration for which the observed retardation of thermodynamically stable aggregates is maximal. Addition of fragmentation and coagulation reactions appears to result in the formation of significantly longer metastable aggregates. We attribute this to the result of two simultaneous competing mechanisms, i.e., on one hand the formation and elongation of X- and Y-type aggregates, and on the other hand the conversion of Y- to X-type aggregates. Fragmentation and coagulation events do not directly contribute to the interconversion, as this exchange exclusively proceeds via the monomer pool and consequently only via monomer associations and dissociations. However, these fragmentation and coagulation events do accelerate the elongation of both assembly types individually, as observed above for the single pathway

DOI: 10.1021/acscentsci.6b00009
ACS Cent. Sci. 2016, 2, 232–241

aggregations. Interconversion of the longer (and thus fewer) Y-type aggregates through subsequent monomer associations and dissociations via the monomer pool then takes longer. The retarded formation of stable assemblies and the increased length of metastable aggregates are also evident in two snapshots (Figure 4f) of stochastic simulations (Movie 5) which capture respectively a system in the absence and one in the presence of fragmentation and coagulation events at the same moment in time after initiation of aggregation (t = 5 s).

2.5. Seeded Supramolecular Polymerizations. Finally, we investigate living supramolecular polymerizations as recently achieved in a biomimetic approach by Ogi et al.[41] In this system, a porphyrin monomer assembles into two different aggregate types, i.e., thermodynamically stable H-aggregates that do not nucleate spontaneously and kinetically trapped J-aggregates. Upon addition of seeds of thermodynamically stable assemblies to a J-aggregate solution, the kinetically trapped aggregates are converted to H-aggregates. Whereas the dynamic nature of supramolecular polymerization usually gives rise to a broad size distribution, the addition of seeds provides kinetic control over initiation of H-aggregate growth resulting in aggregate lengths with low polydispersity. To analyze these living supramolecular polymerizations, we use the same reaction scheme with two parallel operating self-assembly pathways as discussed in the previous section (Figure 4a), though with different parameters. The kinetically controlled assemblies J (instead of Y) increase their size via an isodesmic mechanism (σ = 1) while growth of thermodynamically stable aggregates H (instead of X) proceeds via a highly cooperative nucleation−elongation mechanism (σ = 10^{-9}), preventing spontaneous nucleation within the simulation time.

The seeded supramolecular polymerization is investigated by stochastically simulating the time evolution of the fraction of monomers in cooperative H-aggregates (φ_H) upon addition of various ratios of H-seed solution to an equiconcentrated solution of kinetically trapped J-aggregates (Figure 5a). Upon addition of seeds, aggregation of H-aggregates occurs without a lag time. In case aggregation exclusively proceeds via monomer associations and dissociations, the initial rate of φ_H increase shows a linear relationship with the seed concentration as long as dilution by seed addition is limited, indicating that the supramolecular polymerization is first order with respect to the seed concentration (Figure 5b). A thousand seconds after addition of seeds, H-type aggregates show a narrow length distribution, as evidenced by a calculated polydispersity index (PDI) smaller than 1.01 for each of the seed to J-aggregate ratios. Incorporation of fragmentation and coagulation into the model significantly decreases the rate at which H-aggregates grow upon addition of H-seeds to the kinetically trapped J-aggregates, especially for higher seed to J-aggregate ratios. This reduced growth rate can be attributed to a rapid reduction in the number of seeds, which results from frequent coalescence of seeds in combination with an apparent lack of fragmentation events for the highly cooperative H-aggregates within the time frame of the simulations. Apart from reducing the H-aggregate growth rate, the coagulation events also prevent the formation of narrowly disperse aggregates as evidenced by PDI values larger than 1.7. Comparison to the experiments by Ogi et al.,[41] which show a low PDI as well as a linear relationship between on-pathway product formation and seed ratio, reveals that the kinetics in their system is well described using our model with only monomer associations and dissociations and that, though fragmentations may be frequent in the isodesmic pathway (see Figure S16), spontaneous fragmentation events play no role in the growth of highly cooperative H-aggregates during the experimental time scale.

In order to investigate whether a supramolecular polymerization proceeding exclusively via monomer associations and dissociations allows for the formation of well-controlled supramolecular blockcopolymers, we next repeatedly added equilibrated isodesmic J-aggregates to a system initially exclusively comprising H-type seeds of length 250. The simulated time evolution of φ_H (Figure 5c) shows that the rate of supramolecular polymerization halves each cycle as no new H-aggregates are nucleated within the experimental time scale and each addition of the isodesmic solution halves the concentration of existing H-aggregates. Cumulative histograms of length distributions of H-aggregates at the end of each cycle show that this repeated process results in increasingly longer polymers with controlled lengths and narrow polydispersity (Figure 5d), in agreement with experiments.[41] The mean length of the aggregates roughly doubles each cycle, corresponding with a blockwise growth of the aggregates, indeed allowing for the formation of supramolecular diblock copolymers. Snapshots (Figure 5e) of stochastic simulations (Movie 6) showing two cycles of J-aggregate addition to H-seeds with an initial length of 100 corroborate the blockwise growth in such a process.

3. CONCLUSION

In this study, we have analyzed the effect of spontaneous fragmentation and coagulation reactions on supramolecular polymerizations of increasing mechanistic complexity. While these reactions do not influence the steady-state distribution of aggregate species, they have a large influence on self-assembly kinetics, which may be probed in experimental kinetics studies. Importantly, we reveal the critical relation between molecular cooperativity and the number of fragmentation and coagulation events. Our results show that although with increasing cooperativity the frequency of fragmentation and coagulation events diminishes, the presence of these reactions influences the transient behavior of cooperative one-dimensional self-assemblies even stronger than that of isodesmic aggregates. Moreover, the precise effect of scission and recombination events on the time scale of supramolecular polymerizations sensitively depends on the exact mechanism. It may result in increases (e.g., for the single pathway polymerization and majority rules cases) as well as, much more counterintuitive, decreases (in case of competing pathways) in equilibration kinetics by orders of magnitude. In addition, the simulations provide insight into the effect of multiple, parallel operating self-assembly pathways on one-dimensional aggregation kinetics, a topic of recent interest.[29,32,34,38,41] While in the current simulations fragmentation and coagulation reactions are spontaneous and obey detailed balance, minor modifications would allow us to study fragmentation under nonequilibrium conditions,[52] i.e., by continuous stirring or by applying ultrasound.

4. COMPUTATIONAL METHODS

The effect of fragmentation and coagulation on supramolecular (co)polymerization kinetics has been studied using two techniques: (i) an ordinary differential equations (ODE) approach with one differential equation per aggregate type and length—truncated at a maximum aggregate length N = 2000—and (ii) kinetic Monte Carlo simulations using a variation of the stochastic simulation algorithm (SSA) developed by Gillespie.[66]

DOI: 10.1021/acscentsci.6b00009
ACS Cent. Sci. 2016, 2, 232−241

Both techniques have been selected as both have been used before to investigate supramolecular (co)polymerization kinetics,[29,32−34,39,45,46] both allow for the incorporation of fragmentation and coagulation reactions, and both have their own advantages while providing the same results (up to some stochastic fluctuations). The main advantages of the ODE approach include its deterministic nature and the relatively low computational demand provided the number of ODEs remains limited. In contrast, the main advantages of the kinetic Monte Carlo approach are the absence of a required upper limit to the polymer length, the visualization possibilities as movies, and the computationally feasible extension to multicomponent coaggregation.[29] The systems of differential equations were solved in MATLAB using the standard ode15s solver for stiff differential equations. The stochastic simulations have been performed using an in-house developed dedicated C++-code. Details about the ODEs as well as the stochastic simulation approach are provided in section S1 of the Supporting Information. Forward and backward rate constants, as well as concentrations, have been selected such that aggregation dynamics occurs on the seconds to hours time scale, corresponding to several systems studied experimentally.[28,32,34,41]

■ ASSOCIATED CONTENT

Supporting Information

The Supporting Information is available free of charge on the ACS Publications website at DOI: 10.1021/acscentsci.6b00009.

Details of the derivation and validation of the (co)-polymerization models, figures, and description of supplementary movies (PDF)
Movie 1 (MPG)
Movie 2 (AVI)
Movie 3 (MPG)
Movie 4 (AVI)
Movie 5 (MPG)
Movie 6 (MPG)

■ AUTHOR INFORMATION

Corresponding Authors

*E-mail: a.j.markvoort@tue.nl.
*E-mail: t.f.a.d.greef@tue.nl.

Notes

The authors declare no competing financial interest.

■ ACKNOWLEDGMENTS

We would like to thank E. W. Meijer, P. A. Korevaar, D. van der Zwaag, and A. T. Haedler for fruitful discussions. We acknowledge financial support from The Netherlands Organisation for Scientific Research (NWO): VENI Grant: 722.012.0001 and Gravity program 024.001.035.

■ REFERENCES

(1) Lehn, J. M. Supramolecular polymer chemistry- scope and perspectives. *Polym. Int.* **2002**, *51*, 825−839.
(2) Brunsveld, L.; Folmer, B. J. B.; Meijer, E. W.; Sijbesma, R. P. Supramolecular polymers. *Chem. Rev.* **2001**, *101*, 4071−4097.
(3) Aida, T.; Meijer, E. W.; Stupp, S. I. Functional supramolecular polymers. *Science* **2012**, *335*, 813−817.
(4) De Greef, T. F. A.; Smulders, M. M. J.; Wolffs, M.; Schenning, A. P. H. J.; Sijbesma, R. P.; Meijer, E. W. Supramolecular Polymerization. *Chem. Rev.* **2009**, *109*, 5687−5754.
(5) Yang, L.; Tan, X.; Wang, Z.; Zhang, X. Supramolecular polymers: historical development, preparation, characterization, and functions. *Chem. Rev.* **2015**, *115*, 7196−7239.
(6) van der Zwaag, D.; de Greef, T. F. A.; Meijer, E. W. Programmable supramolecular polymerizations. *Angew. Chem., Int. Ed.* **2015**, *54*, 8334−8336.
(7) Palmer, L. C.; Stupp, S. I. Molecular self-assembly into one-dimensional nanostructures. *Acc. Chem. Res.* **2008**, *41*, 1674−1684.
(8) Shah, R. N. Supramolecular design of self-assembling nanofibers for cartilage regeneration. *Proc. Natl. Acad. Sci. U. S. A.* **2010**, *107*, 3293−3298.
(9) Zhang, S. Fabrication of novel biomaterials through molecular self-assembly. *Nat. Biotechnol.* **2003**, *21*, 1171−1178.
(10) Zhang, W.; Jin, W.; Fukushima, T.; Saeki, A.; Seki, S.; Aida, T. Supramolecular linear heterojunction composed of graphite-like semiconducting nanotubular segments. *Science* **2011**, *334*, 340−343.
(11) Haedler, A. T.; Kreger, K.; Issac, A.; Wittmann, B.; Kivala, M.; Hammer, N.; Köhler, J.; Schmidt, H.; Hildner, R. Long-range energy transport in single supramolecular nanofibres at room temperature. *Nature* **2015**, *523*, 196−199.
(12) Winiger, C. B.; Li, S.; Kumar, G. R.; Langenegger, S. M.; Häner, R. Long-distance electronic energy transfer in light-harvesting supramolecular polymers. *Angew. Chem., Int. Ed.* **2014**, *53*, 13609−13613.
(13) Zang, L.; Che, Y.; Moore, J. S. One-dimensional self-assembly of planar π-conjugated molecules: adaptable building blocks for organic nanodevices. *Acc. Chem. Res.* **2008**, *41*, 1596−1608.
(14) Burnworth, M.; Tang, L.; Kumpfer, J. R.; Duncan, A. J.; Beyer, F. L.; Fiore, G. L.; Rowan, S. J.; Weder, C. Optically healable supramolecular polymers. *Nature* **2011**, *472*, 334−338.
(15) Yan, X.; Wang, F.; Zheng, B.; Huang, F. Stimuli-responsive supramolecular polymeric materials. *Chem. Soc. Rev.* **2012**, *41*, 6042−6065.
(16) Rybtchinski, B. Adaptive supramolecular nanomaterials based on strong noncovalent interactions. *ACS Nano* **2011**, *5*, 6791−6818.
(17) Chen, Z.; Lohr, A.; Saha-Möller, C. R.; Würthner, F. Self-assembled π-stacks of functional dyes in solution: structural and thermodynamic features. *Chem. Soc. Rev.* **2009**, *38*, 564−584.
(18) Martin, R. B. Comparisons of indefinite self-association models. *Chem. Rev.* **1996**, *96*, 3043−3064.
(19) Jonkheijm, P.; van der Schoot, P.; Schenning, A. P. H. J.; Meijer, E. W. Probing the solvent-assisted nucleation pathway in chemical self-assembly. *Science* **2006**, *313*, 80−83.
(20) Zhao, D.; Moore, J. S. Nucleation−elongation: a mechanism for cooperative supramolecular polymerization. *Org. Biomol. Chem.* **2003**, *1*, 3471−3491.
(21) Kulkarni, C.; Balasubramanian, S.; George, S. J. What molecular features govern the mechanism of supramolecular polymerization? *ChemPhysChem* **2013**, *14*, 661−673.
(22) Rest, C.; Kandanelli, R.; Fernández, G. Strategies to create hierarchical self-assembled structures via cooperative non-covalent interactions. *Chem. Soc. Rev.* **2015**, *44*, 2543−2572.
(23) Douglas, J. F.; Dudowicz, J.; Freed, K. F. Lattice model of equilibrium polymerization. VII. Understanding the role of "cooperativity" in self-assembly. *J. Chem. Phys.* **2008**, *128*, 224901.
(24) Nakano, Y.; Markvoort, A. J.; Cantekin, S.; Filot, I. A. W.; ten Eikelder, H. M. M.; Meijer, E. W.; Palmans, A. R. A. Conformational Analysis of Chiral Supramolecular Aggregates: Modeling the Subtle Difference between Hydrogen and Deuterium. *J. Am. Chem. Soc.* **2013**, *135*, 16497−16506.
(25) Van Workum, K.; Douglas, J. F. Symmetry, equivalence, and molecular self-assembly. *Phys. Rev. E* **2006**, *73*, 031502.
(26) Buchelnikov, A. S.; Evstigneev, V. P.; Evstigneev, M. P. General statistical-thermodynamical treatment of one-dimensional multicomponent molecular hetero-assembly in solution. *Chem. Phys.* **2013**, *421*, 77−83.
(27) Jabbari-Farouji, S.; van der Schoot, P. P. A. M. Theory of supramolecular co-polymerization in a two-component system. *J. Chem. Phys.* **2012**, *137*, 064906.

DOI: 10.1021/acscentsci.6b00009
ACS Cent. Sci. 2016, 2, 232−241

(28) Smulders, M. M. J.; Filot, I. A. W.; Leenders, J. M. A.; van der Schoot, P.; Palmans, A. R. A.; Schenning, A. P. H. J.; Meijer, E. W. Tuning the Extent of Chiral Amplification by Temperature in a Dynamic Supramolecular Polymer. *J. Am. Chem. Soc.* **2010**, *132*, 611−619.
(29) Markvoort, A. J.; ten Eikelder, H. M. M.; Hilbers, P. A. J.; de Greef, T. F. A.; Meijer, E. W. Theoretical models of nonlinear effects in two-component cooperative supramolecular copolymerizations. *Nat. Commun.* **2011**, *2*, 509.
(30) ten Eikelder, H. M. M.; Markvoort, A. J.; de Greef, T. F. A.; Hilbers, P. A. J. An Equilibrium Model for Chiral Amplification in Supramolecular Polymers. *J. Phys. Chem. B* **2012**, *116*, 5291−5301.
(31) Pashuck, E. T.; Stupp, S. I. Direct observation of morphological transformation from twisted ribbons into helical ribbons. *J. Am. Chem. Soc.* **2010**, *132*, 8819−8821.
(32) Korevaar, P. A.; George, S. J.; Markvoort, A. J.; Smulders, M. M. J.; Hilbers, P. A. J.; Schenning, A. P. H. J.; de Greef, T. F. A.; Meijer, E. W. Pathway complexity in supramolecular polymerization. *Nature* **2012**, *481*, 492−496.
(33) Baram, J.; Weissman, H.; Rybtchinski, B. Supramolecular polymer transformation: a kinetic study. *J. Phys. Chem. B* **2014**, *118*, 12068−12073.
(34) van der Zwaag, D.; Pieters, P. A.; Korevaar, P. A.; Markvoort, A. J.; Spiering, A. J. H.; de Greef, T. F. A.; Meijer, E. W. Kinetic analysis as a tool to distinguish pathway complexity in molecular assembly: an unexpected outcome of structures in competition. *J. Am. Chem. Soc.* **2015**, *137*, 12677−12688.
(35) Mattia, E.; Otto, S. Supramolecular systems chemistry. *Nat. Nanotechnol.* **2015**, *10*, 111−119.
(36) Sciortino, F.; Bianchi, E.; Douglas, J. F.; Tartaglia, P. Self-assembly of patchy particles into polymer chains: A parameter-free comparison between Wertheim theory and Monte Carlo simulation. *J. Chem. Phys.* **2007**, *126*, 194903.
(37) Korevaar, P. A.; de Greef, T. F. A.; Meijer, E. W. Pathway complexity in π-conjugated materials. *Chem. Mater.* **2014**, *26*, 576−586.
(38) Ogi, S.; Fukui, T.; Jue, M. L.; Takeuchi, M.; Sugiyasu, K. Kinetic control over pathway complexity in supramolecular polymerization through modulating the energy landscape by rational molecular design. *Angew. Chem., Int. Ed.* **2014**, *53*, 14363−14367.
(39) Levin, A.; Mason, T. O.; Adler-Abramovich, L.; Buell, A. K.; Meisl, G.; Galvagnion, C.; Bram, Y.; Stratford, S. A.; Dobson, C. M.; Knowles, T. P. J.; Gazit, E. Ostwald's rule of stages governs structural transitions and morphology of dipeptide supramolecular polymers. *Nat. Commun.* **2014**, *5*, 5219.
(40) Wang, X.; Guerin, G.; Wang, H.; Wang, Y.; Manners, I.; Winnik, M. A. Cylindrical block copolymer micelles and co-micelles of controlled length and architecture. *Science* **2007**, *317*, 644−647.
(41) Ogi, S.; Sugiyasu, K.; Manna, S.; Samitsu, S.; Takeuchi, M. Living supramolecular polymerization realized through a biomimetic approach. *Nat. Chem.* **2014**, *6*, 188−195.
(42) Ogi, S.; Stepanenko, V.; Sugiyasu, K.; Takeuchi, M.; Würthner, F. Mechanism of self-assembly process and seeded supramolecular polymerization of perylene bisimide organogelator. *J. Am. Chem. Soc.* **2015**, *137*, 3300−3307.
(43) Görl, D.; Zhang, X.; Stepanenko, V.; Würthner, F. Supramolecular block copolymers by kinetically controlled co-self-assembly of planar and core-twisted perylene bisimides. *Nat. Commun.* **2015**, *6*, 7009.
(44) Kang, J.; Miyajima, D.; Mori, T.; Inoue, Y.; Itoh, Y.; Aida, T. A rational strategy for the realization of chain-growth supramolecular polymerization. *Science* **2015**, *347*, 646−651.
(45) Lohr, A.; Würthner, F. Evolution of homochiral helical dye assemblies: involvement of autocatalysis in the 'majority-rules' effect. *Angew. Chem., Int. Ed.* **2008**, *47*, 1232−1236.
(46) Korevaar, P. A.; Grenier, C.; Markvoort, A. J.; Schenning, A. P. H. J.; de Greef, T. F. A.; Meijer, E. W. Model-driven optimization of multicomponent self-assembly process. *Proc. Natl. Acad. Sci. U. S. A.* **2013**, *110*, 17205−17210.
(47) Cantekin, S.; ten Eikelder, H. M. M.; Markvoort, A. J.; Veld, M. A.; Korevaar, P. A.; Green, M. M.; Palmans, A. R. A.; Meijer, E. W. Consequences of cooperativity in racemizing supramolecular systems. *Angew. Chem., Int. Ed.* **2012**, *51*, 6426−6431.
(48) Oosawa, F.; Kasai, M. A Theory of linear and helical aggregations of macromolecules. *J. Mol. Biol.* **1962**, *4*, 10−21.
(49) Goldstein, R. F.; Stryer, L. Cooperative polymerization reactions. Analytical approximations, numerical examples, and experimental strategy. *Biophys. J.* **1986**, *50*, 583−599.
(50) Powers, E. T.; Powers, D. L. The kinetics of nucleated polymerizations at high concentrations: amyloid fibril formation near and above the "supercritical concentration". *Biophys. J.* **2006**, *91*, 122−132.
(51) Powers, E. T.; Powers, D. L. Mechanisms of protein fibril formation: nucleated polymerization with competing off-pathway aggregation. *Biophys. J.* **2008**, *94*, 379−391.
(52) Carnall, J. M. A.; Waudby, C. A.; Belenguer, A. M.; Stuart, M. C. A.; Peyralans, J. J. P.; Otto, S. Mechanosensitive self-replication driven by self-organization. *Science* **2010**, *327*, 1502−1506.
(53) Schulman, R.; Yurke, B.; Winfree, E. Robust self-replication of combinatorial information via crystal growth and scission. *Proc. Natl. Acad. Sci. U. S. A.* **2012**, *109*, 6405−6410.
(54) Knowles, T. P. J.; Waudby, C. A.; Devlin, G. L.; Cohen, S. I. A.; Aguzzi, A.; Vendruscolo, M.; Terentjev, E. M.; Welland, M. E.; Dobson, C. M. An analytical solution to the kinetics of breakable filament assembly. *Science* **2009**, *326*, 1533−1537.
(55) Cohen, S. I. A.; Linse, S.; Luheshi, L. M.; Hellstrand, E.; White, D. A.; Rajah, L.; Otzen, D. E.; Vendruscolo, M.; Dobson, C. M.; Knowles, T. P. J. Proliferation of Aβ40 and Aβ42 aggregates occurs through a secondary nucleation mechanism. *Proc. Natl. Acad. Sci. U. S. A.* **2013**, *110*, 9758−9763.
(56) Xue, W. F.; Homans, S. W.; Radford, S. E. Systematic analysis of nucleation-dependent polymerization reveals new insights into the mechanism of amyloid self-assembly. *Proc. Natl. Acad. Sci. U. S. A.* **2008**, *105*, 8926−8931.
(57) Gillam, J. E.; MacPhee, C. E. Modelling amyloid fibril formation kinetics: mechanisms of nucleation and growth. *J. Phys.: Condens. Matter* **2013**, *25*, 373101.
(58) Michaels, T. C. T.; Knowles, T. P. J. Role of filament annealing in the kinetics and thermodynamics of nucleated polymerization. *J. Chem. Phys.* **2014**, *140*, 214904.
(59) Cates, M. E.; Candau, S. J. Statics and dynamics of worm-like surfactant micelles. *J. Phys.: Condens. Matter* **1990**, *2*, 6869−6892.
(60) Nyrkova, I. A.; Semenov, A. N. (2005). On the theory of micellization kinetics. *Macromol. Theory Simul.* **2005**, *14*, 569−585.
(61) O'Shaughnessy, B.; Yu, J. Rheology of Wormlike Micelles: Two Universality Classes. *Phys. Rev. Lett.* **1995**, *74*, 4329−4332.
(62) Padding, J. T.; Boek, E. S. Evidence for diffusion-controlled recombination kinetics in model wormlike micelles. *Europhys. Lett.* **2004**, *66*, 756−762.
(63) Huang, C. C.; Xu, H.; Ryckaert, J. P. Kinetics and dynamic properties of equilibrium polymers. *J. Chem. Phys.* **2006**, *125*, 094901.
(64) Van Dongen, P. G. J.; Ernst, M. H. Kinetics of reversible polymerization. *J. Stat. Phys.* **1984**, *37*, 301−324.
(65) Green, M. M.; Peterson, N. C.; Sato, T.; Teramoto, A. A helical polymer with a cooperative response to chiral information. *Science* **1995**, *268*, 1860−1866.
(66) Gillespie, D. T. Exact stochastic simulation of coupled chemical reactions. *J. Phys. Chem.* **1977**, *81*, 2340−2361.

DOI: 10.1021/acscentsci.6b00009
ACS Cent. Sci. 2016, 2, 232−241